Exact diagonalization of pure $\mathbb{Z}_2$ gauge theory

Quantum Simulation of Gauge Theories - End-of-Semester Project

Thomas Leplumey

December 11, 2023

ETH zürich

Contents

Introduction **2**

1 Theoretical aspects of pure $\mathbb{Z}_2$ gauge theory in $(2+1)$d **2**
1.1 Hamiltonian formulation . . . 2
1.2 Gauge invariance . . . 2
1.3 Description of the physical space . . . 3

2 Exact diagonalization on the lattice **5**
2.1 Power methods . . . 5
2.2 Restriction to the physical space . . . 5

3 Analysis of the energy spectrum **6**

4 Time evolution **6**
4.1 Computational considerations . . . 6
4.2 Example of application . . . 7

5 Conclusion and future prospects **9**

Bibliography **10**

Introduction

The goal of this report is to present the practical resolution of a quantum field theory on the lattice, through the method of exact diagonalization. The pure $\mathbb{Z}_2$ gauge theory in $(2+1)$ has been chosen for this demonstration, since it presents many of the interesting aspects of gauge theories but remains simple enough to be exact diagonalized. We will first describe how one can take advantage of the gauge invariance of the theory to greatly simplify the problem, with a set of considerations that can be generalized to even more complicated gauge theories. Then we will explain how the theory and its exact diagonalization is realized in practice. Finally, after applying the diagonalization on 2×2 and 3×3 lattices, we will quickly analyze the energy spectrum obtained and present an example of application to compute the time evolution of some observables.

The whole code used in this work can be found in this github repository [4].

1 Theoretical aspects of pure $\mathbb{Z}_2$ gauge theory in $(2+1)$d

1.1 Hamiltonian formulation

As described, for instance, in [5] and [2], pure $\mathbb{Z}_2$ gauge theory in $(2+1)$ dimensions consists in a gauge theory of gauge group $\mathbb{Z}_2$ on a square lattice, considering only gauge fields. Thus our only degrees of freedom live on the links, and can only take values ±1. We can thus represent them by Pauli matrix σ^z. The kinetic term in the Hamiltonian then takes the usual form:

$$\mathcal{H}_K = -K \sum_{\square} \prod_{\ell \in \square} \sigma^z_\ell$$

where $\square$ are the plaquettes of the lattice, and ℓ the links.

Furthermore, as we will see in the following section, we are allowed to add another term to the hamiltonian without breaking gauge invariance nor the discrete translation symmetry, which leads to the complete hamiltonian:

$$\mathcal{H} = -K \sum_{\square} \prod_{\ell \in \square} \sigma^z_\ell - g \sum_{\ell} \sigma^x_\ell$$

1.2 Gauge invariance

The transformation of the link variables is as usual:

$$\sigma^z_{n,\hat{u}} \longrightarrow \Omega(n) \sigma^z_{n,\hat{u}} \Omega(n+\hat{u})$$

where n is a vertex position on the lattice, $\hat{u}$ is one of the 2 positive unit vectors $(1,0)$ and $(0,1)$, and Ω has values in $\mathbb{Z}_2$.

In particular, let's consider for a given n_0 the local gauge transformation $\Omega(n_0) = -1$ and $\Omega(n) = 1$ for $n \neq n_0$. Then, only the 4 links attached to n_0 will be flipped, and the other links remain unchanged. Since the flip of σ^z can be described by the action of the other Pauli matrix σ^x, we can write this local gauge transformation as:

$$G(n_0) = \prod_{n_0 \in \ell} \sigma^x_\ell$$

For a complete proof, we can check that $G(n_0)\sigma^z_\ell G(n_0) = \rho_\ell \sigma^z_\ell$ with $\rho_\ell = -1$ if $n_0 \in \ell$ and $\rho_\ell = 1$ otherwise, which corresponds to the transformation of the links written above. As expected, it follows that all the $G(n_0)$ commute with the kinetic Hamiltonian $\mathcal{H}_K$, proving that our theory is $\mathbb{Z}_2$ gauge invariant. We can then fix the gauge by imposing for all n:

$$G(n) = 1$$

But surprisingly, due to the periodicity of the lattice, some other gauge transformations remain that cannot be expressed with the $G(n)$ operators. We will call these transformations "topological", as they only depend on the topology of the lattice (toric in our case). Consider for example the transformation V_x (x denotes the direction on the square lattice here), which is the product of all the σ^x matrices on the links pierced by the path $\bar{\mathcal{C}}_x$ (c.f. Figure 2).

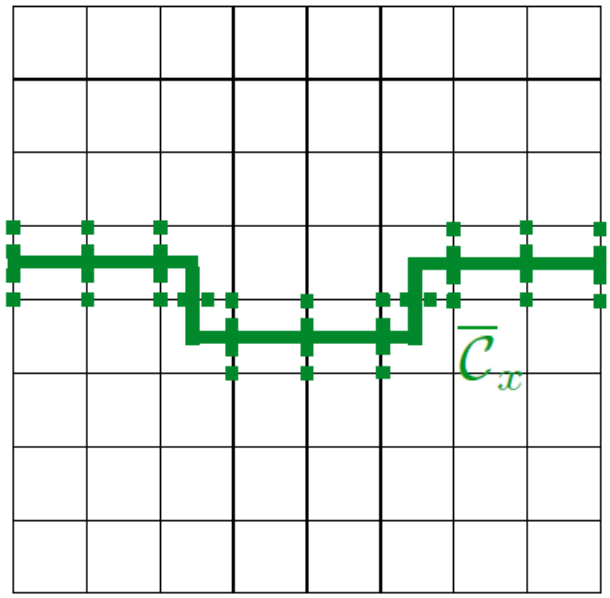

Figure 2: Illustration of the topological transformation V_x.

One might also consider paths turning multiple times around the torus in both directions However it turns out that these transformations are not independent due to prior gauge fixing. As a result, there are only two unique topological transformations, denoted as V_x and V_y.

1.3 Description of the physical space

Now let's quickly analyze the dimension of our system. Let L^2 be the number of vertices on the lattice (with periodic boundary conditions). Thus, there are $2L^2$ links, resulting in a Hilbert space of dimension $d = 2^{2L^2}$.

We have L^2 local gauge fixing conditions (one per vertex), but only $L^2 - 1$ independent ones (since the product of all the $G(n)$ is the identity). Furthermore, we also have 2 independent topological

Lattice size	Full Hilbert space	Physical space
L	2^{2L^2}	2^{L^2-1}
1	4	1
2	256	8
3	262 144	256
4	4 294 967 296	32 768

Table 1: Dimensions of the Hilbert spaces for different lattice sizes

gauge fixing conditions. Therefore, the dimension of the Hilbert space describing the physical sector is then:

$$d_{ph}(L) = \frac{2^{2L^2}}{2^{L^2-1} \times 2^2} = 2^{L^2-1}$$

Table 1 shows the dimension of the full Hilbert space and the dimension of the physical Hilbert space for several lattice sizes. The reader can appreciate the very significant gain, keeping in mind the perspective of exact diagonalization.

We now want to construct a basis of this physical state. Furthermore, we will construct an eigenbasis of the non-interacting Hamiltonian $\mathcal{H}_K$, which will be useful in the following. Thanks to the removal of all gauge redundancies, the free vacuum is longer degenerate in the physical state. One can convince himself that the state $|\Uparrow\rangle$ with all spins up is a ground state of $\mathcal{H}_K$. It does not belong to the physical space, we can easily project it on it and thus find our unique free vacuum state:

$$|0\rangle = (\mathbb{1} + V_x)(\mathbb{1} + V_y) \prod_n (\mathbb{1} + G(n)) \, |\Uparrow\rangle$$

Then, to excite the vacuum state, we can flip some links with σ_x matrices. More precisely, flipping all the spins along a path creates $\mathbb{Z}_2$ fluxes of -1 on the two plaquettes at the ends of the path, which are called *visions* [5], as shown in Figure 3. This excited state is still an eigenstate of $\mathcal{H}_K$, and the energy of such a state is thus $4K$ above the vacuum energy (because of two plaquettes passing from $\mathbb{Z}_2$ flux 1 to $\mathbb{Z}_2$ flux -1).

We can then create one excited state for each even set of plaquettes, with each state being a multiple of $4K$ above the vacuum energy. Given there are L^2 plaquettes, this procedure generates a number of states equal to:

$$\sum_{k=0}^{\lfloor L^2/2 \rfloor} \binom{L^2}{2k} = 2^{L^2-1} = d_{ph}$$

This ensures that we have generated a complete basis of the physical space. Even though it is an eigenbasis only of the free hamiltonian $\mathcal{H}_K$, it remains a basis of the physical space anyway, which will be useful later to project all our observables on the physical space.

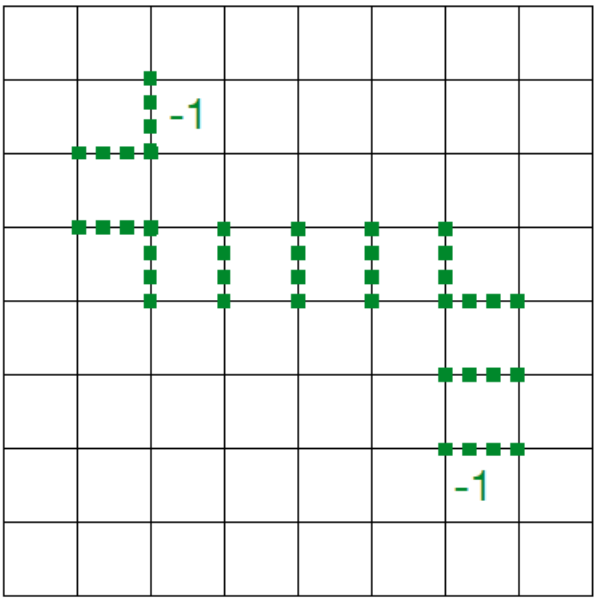

Figure 3: Illustration of a state with two visions. σ^x matrices are applied on the green links, so that a $\mathbb{Z}_2$ flux of -1 remains on the two plaquettes at the ends of the path.

2 Exact diagonalization on the lattice

2.1 Power methods

In practice, the determination of the eigenvalues of a hermitian matrix $\mathcal{H}$ is based on the simple observation that $\mathcal{H}^n |\psi\rangle$ grows asymptotically as $(E_{max})^n |E_{max}\rangle$, with E_{max} the largest eigenvalue (in modulus) and $|E_{max}\rangle$ the associated eigenvector. The method we use here is called **Lanczos Angorithm** [1], and its implementation in **Arpack** [3], which is based on this principle, but also incorporates other tricks for better convergence and numerical stability.

2.2 Restriction to the physical space

With the procedure presented in Section 1.3, we can construct in practice a basis of the physical space that diagonalizes the free hamiltonian $\mathcal{H}_K$. Let $\mathcal{B}$ this basis, which can be seen as a $d \times d_{ph}$ matrix. Then, we can project the hamiltonian on the physical space as:

$$\tilde{\mathcal{H}} = \mathcal{B}^\top \mathcal{H} \mathcal{B}$$

In practice, it is more convenient to project the two terms of the hamiltonian separately, so that we can change the parameters easily in the following without computing these heavy matrix products each time but only a sum of two small matrices.

$\tilde{\mathcal{H}}$ is now a $d_{ph} \times d_{ph}$ matrix, suitable for being diagonalized. Once we get our eigenvectors $|E\rangle_{ph}$ in the physical basis, we can easily go back to the full Hilbert space by computing:

$$|E\rangle = \mathcal{B} |E\rangle_{ph}$$

3 Analysis of the energy spectrum

Now that we can easily compute a full eigenbasis of our hamiltonian for any set of parameters, we can look at the dependance of the spectrum in these parameters. For simplicity, let's fix $K = 1$ as we don't want to change our kinetic hamiltonian, and vary g from 0 to large values. Figure 4 shows the variation of the spectrum as a function of g for $L = 2$ and $L = 3$.

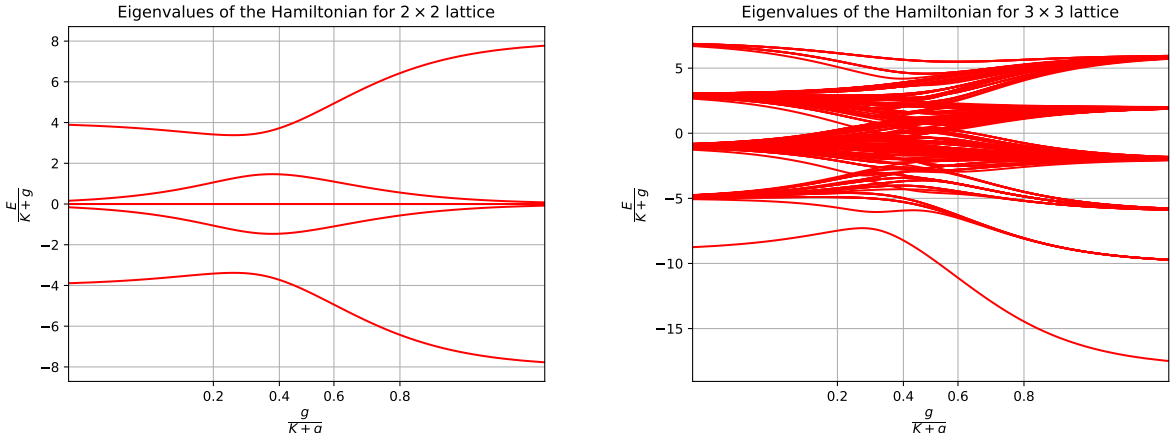

Figure 4: Dependence on g of the eigenvalues for 2×2 lattice (left) and 3×3 lattice (right). The x and y axis are normalized by $K + g$, and the x axis is scaled by a sigmoid function, so that the behaviour at low g and large g is more readable.

We observe, as expected, that for $g = 0$, only the energies $(-L^2 + 4n)K$ are filled and highly degenerate (the degeneracy corresponding to the binomial coefficients, as shown in 1.3). For $g \ll K$, the degeneracy is partially lifted around the free eigenvalues, while for $g \gg K$ they organize again around the values $(-2L^2 + 4n)g$ (not all filled).

To understand this last asymptotic behaviour qualitatively, we can simply look at the hamitonian with $K = 0$. In that case, the ground state is the state in which all the spins have $\sigma_x = 1$, with eigenvalue $-2L^2 g$. Then, the only way to excite this state while remaining in the physical state is to apply products of σ^z matrices on a closed loop (that can eventually cross the borders but only an even number of times because of the topological gauge fixing conditions), as illustrated in Figure 5. Such products necessarily have an even number of σ^z factors, which explains that only the levels $(-2L^2 + 4n)g$ are allowed. Furthermore, we see for example that it is impossible to form a loop with only two links, which explains why the $n = 1$ level is empty.

4 Time evolution

4.1 Computational considerations

One of the main interests of having the Hamiltonian diagonalized is that we can compute the time evolution of any initial state $|\psi_0\rangle$ at any time t in constant computational time. Indeed, the time evolution $|i\rangle$ is given by:

$$|\psi(t)\rangle = e^{-i\mathcal{H}t} |\psi_0\rangle$$

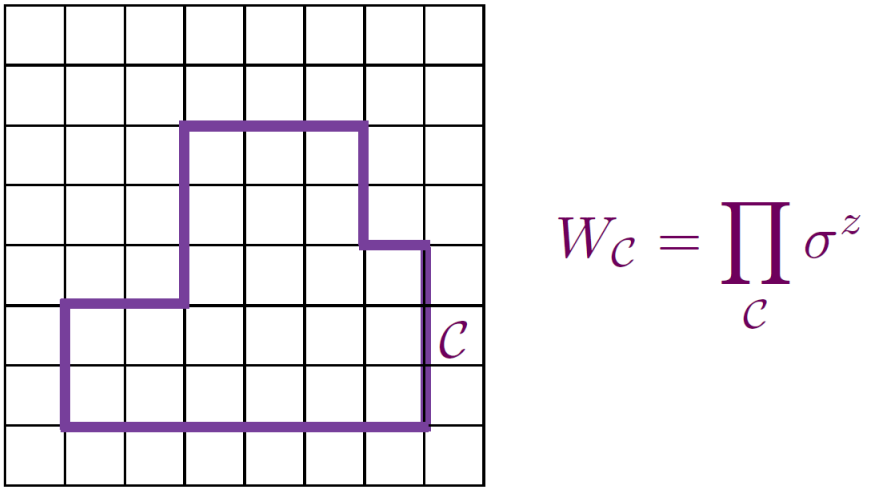

Figure 5: Closed loop of σ^z matrices (Wilson loop), used to excite the ground state in $K = 0$ case.

which, using the eigenbasis, is rewritten as:

$$|\psi(t)\rangle = \sum_{|E\rangle \in \mathcal{B}} e^{-iEt} \langle E|\psi_0\rangle |E\rangle$$

This calculation only involves d_{ph} scalar products of d_{ph}-dimensional vectors once, and d_{ph} scalar exponentiations for every time t, which is very cheap computationally.

4.2 Example of application

In this section, we look at an example of application of time evolution in $\mathbb{Z}_2$ gauge theory. Since we do not want to introduce additional concepts and formalism here, we will apply it to the visions states presented above.

We know that for the free hamiltonian $\mathcal{H}_K$, the eigenstates are the the "vision" excitations of the vacuum, generated with products of σ^x matrices along paths, as explained in Section 1.3. For a general hamiltonian, we can still consider these vision states as the observable states, but they are not eigenstates of the hamiltonian anymore, and thus they can evolve to other states. We are interested here in the time evolution of these states, as a function of the interaction strength g. In all the following, we fix $K = 1$ and $L = 3$.

First, to get an idea of the physical behaviour of our system, Figure 6 shows probability of observing different (even) number of visions from the vacuum state. We can see that for a weak g, the pair states are favored as expected, given the energy cost depends on the number of visions, but for strong g the visions become less costly energetically, and the probabilities stabilize according to the number of configurations for each number of visions.

Now, given our Hamiltonian is fully diagonalized, it is possible to study the time evolution of any initial state in constant computation time. For instance, let's take the state with no visions as our initial state (i.e. the ground state of the free hamiltonian, but not of the full hamiltonian). We can

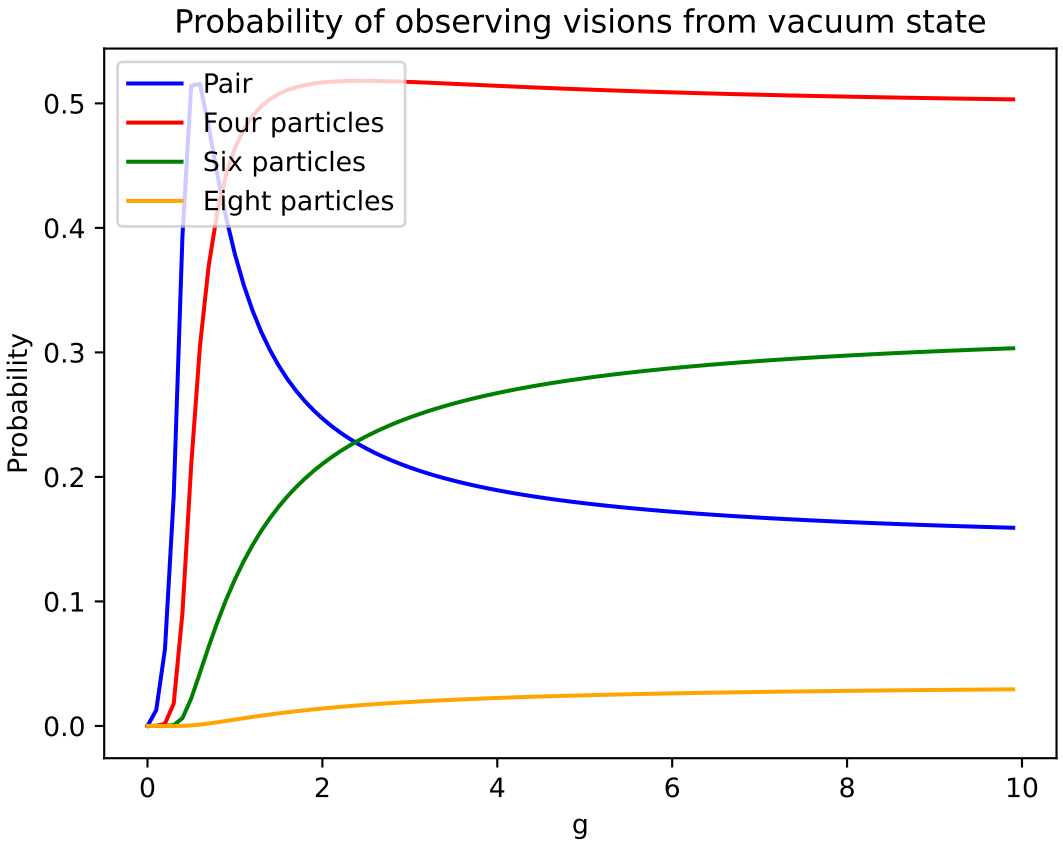

Figure 6: Probabilities of observing different number of visions from the vacuum state, as functions of g

be interested in the number of visions that can spontaneously appear from this state after letting it evolve during a certain time t. This can be computed as follows:

$$\langle N(t)\rangle = \sum_{n\in\mathbb{N}} n \sum_{|u\rangle\in\mathcal{B}_{\text{free}}^{(n)}} \langle u|\psi(t)\rangle$$

with $\mathcal{B}_{\text{free}}^{(n)}$ the set of the states of the free basis with n visions, or we can also simply recall that the number of visions is related to the kinetic energy by:

$$N = \frac{1}{2}\left(\mathcal{H}_K + L\right)$$

Figure 7 shows, for different values of g, the time evolution of the average number of visions, from an initial state with no visions. We see that for very low values of g, this number naturally very close to 0, but for larger values of g this number can reach values up to $\approx \dfrac{L}{2} = 4.5$ and presents pseudo-oscillations. The frequency of these pseudo-oscillations asymptotically scales as $\omega \sim g$ which is expected, but the exact behaviour of the evolution in the phase transition ($g \sim 1$) can only be determined by the exact diagonalization. Furthermore, even in the case $g \gg 1$, for any finite

g, if t is large enough the evolution will deviate from the asymptotic one and in that case exact diagonalisation is also useful.

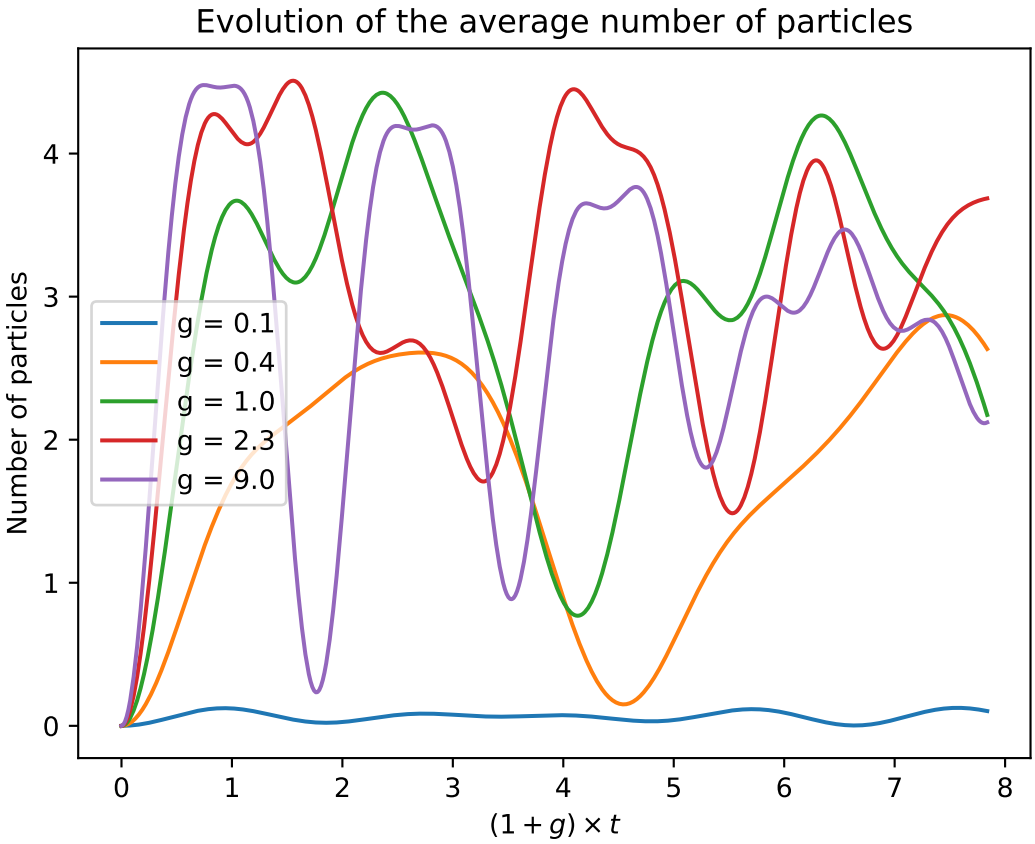

Figure 7: Time evolution of the average number of visions from initial state with no visions, and for different values of g (with fixed $K = 1$, $L = 3$)

5 Conclusion and future prospects

We have seen in this study that both gauge invariance and pure gauge aspects of the theory bring a lot of constraints which allow to considerably reduce the dimension of the physical system. Thanks to these aspects, exact diagonalization on the 2×2 and 3×3 lattices becomes very manageable in small computational time, and one could expect to perform the diagonalization as well on the 4×4 lattice with a little bit more time.

The spectrum obtained after diagonalization has been analysed qualitatively and is physically consistent with what we expect in the two extreme cases $g \ll 1$ and $g \gg 1$. A smooth transition is observed between these two phases, in which the exact diagonalization becomes very useful.

Finally, in analogy to what one could seek to compute in usual quantum field theories, we give an example of time evolution of an observable in the context of visions states, which allows to see

different behaviours for different interaction strengths. This process can be completely generalized to any observable, and the attached notebook [4] provides all the tools to do so.

As a future prospect, one could also expect to take advantage as well of the $(\mathbb{Z}_L)^2$ translation symmetry, $\mathbb{Z}_4$ rotation symmetry and $\mathbb{Z}_2$ parity symmetry to reduce the number of eigenstates to compute effectively, and thus reach higher lattice sizes for this theory.

References

[1] Jane K Cullum and Ralph A Willoughby. *Lanczos algorithms for large symmetric eigenvalue computations: Vol. I: Theory*. SIAM, 2002.

[2] Eduardo Fradkin. *Field theories of condensed matter physics*. Cambridge University Press, 2013.

[3] Richard B Lehoucq, Danny C Sorensen, and Chao Yang. *ARPACK users' guide: solution of large-scale eigenvalue problems with implicitly restarted Arnoldi methods*. SIAM, 1998.

[4] Thomas Leplumey. *Exact diagonalization of pure $\mathbb{Z}_2$ gauge theory*. Dec. 2023.

[5] Sachdev Subir. *$\mathbb{Z}_2$ gauge theory*. Harvard University, 2018.